employed is the precession time appropriate to total (i.e., $T=0$) magnetization. The main peak decays slowly with no hint of structure, within the scatter, in its tail. This is in agreement with Windsor's results, which displayed[21] no structure for infinite temperature. The [100] correlation function (not plotted) displays the main peak, with its maximum at $\tau=1$, and a similar smooth decay. Results obtained for more distant pairs display little above the noise. One obtains, from these results, a spin propagation velocity which is roughly half the value at $T=0$.

The suggestion of a characteristic spin-diffusion or group velocity was first raised by the results of Fig. 8. There was also some suggestion that this description oversimplifies the situation since structure was seen in the [$nn0$] and [nnn] functions at times less than the characteristic transit time of the "main"peak. A study of the spin diffusion associated with one displaced spin in an otherwise ferromagnetic array sheds some light on this. The evolution of such a system is displayed in Fig. 14. A spin at the center of a $16\times16\times16$ sample was initially pointed in the x direction; all others were ferromagnetically aligned in the z direction. The x and y components of a (100) plane of spins, including the displaced spin, are plotted in the figure as a function of time (note the factor of $7\frac{1}{2}$ change in scale between the second and third frames). Assuming a characteristic spin-diffusion or group velocity, one would expect a spherical wave front for the disturbances; in this plane it is square. Further samplings in the (110) plane (which we do not plot) show the disturbance to have a cubic wave front. The velocity of motion of the centers of this front is that already seen in Fig. 8. Such a result is not characteristic of a simple spin-diffusion process but it is consistent with the predictions of spin-wave theory for the case of one infinitesimally perturbed spin. Derivations, similar to those yielding Eq. (13) (see also Huber[13]), give

$$\langle \mathbf{S}_\perp{}^0(0)\cdot\mathbf{S}_\perp{}^{[hkl]}(\tau)\rangle \sim i^{h+k+l}J_h(\tfrac{1}{3}\tau)J_k(\tfrac{1}{3}\tau)J_l(\tfrac{1}{3}\tau)\,, \quad (23)$$

where the internal perturbation takes place at site 0 and at time $\tau=0$. The tendency to square wave fronts, the nodal lines, and the relative phases of 90° of adjacent spins which appear in Fig. 14 are consistent with this equation. The structure seen in the time-displaced correlations is thus predicted by spin-wave theory and it depends strongly on the topology of the simple cubic lattice [as manifested, for example, in the spin-wave dispersion curve, Eq. (8)]. The characteristic velocity seen in Fig. 8 is not simply that of a spin-diffusion process, and the structure which appears prior to the arrival of the main peak is to be expected.

[21] C. G. Windsor, Proc. Phys. Soc. (London) **91**, 353 (1967); see also C. G. Windsor, G. A. Briggs, and M. Kestigian, J. Phys. **C1**, 940 (1968).

ACKNOWLEDGMENTS

We would like to thank Miss E. Wolfson for assistance with the computer programming and G. A. Baker, M. E. Fisher, N. D. Mermin, P. C. Martin, P. Schofield, and S. A. Goudsmit for useful discussions.

PHYSICAL REVIEW VOLUME 181, NUMBER 2 10 MAY 1969

Temperature Dependence of the Susceptibility Tensor of a Weak Ferromagnet: $YFeO_3$†

G. Gorodetsky, S. Shtrikman, Y. Tenenbaum, and D. Treves
Department of Electronics, The Weizmann Institute of Science, Rehovot, Israel
(Received 28 October 1968)

The magnetic susceptibility of $YFeO_3$ has been measured in the temperature range 4.2–1000°K. The temperature dependence of the susceptibility is also derived theoretically using a Heisenberg Hamiltonian and applying the molecular-field approximation. In addition to nearest-neighbor isotropic exchange, antisymmetric exchange, and uniaxial anisotropy terms, a cubic anisotropy term is also included in the Hamiltonian in an attempt to account for the observed temperature variation of the susceptibility parallel to the antiferromagnetic axis. This model explains qualitatively the main features of the experimental results. Using the same model, the third-order term in the field dependence of the magnetization is calculated for $T=0$°K. It follows that, owing to the cubic anisotropy term, quantitative agreement is obtained with the observed departure from linearity in the field dependence of the magnetization, which was measured at 4.2°K and magnetic fields in the range 0–50 kOe.

I. INTRODUCTION

THE orthoferrites RFeO$_3$ (R is a rare earth or yttrium) belong to a class of weak ferromagnets with a slightly distorted perovskite crystallographic structure (space group $D_{2h}{}^{16}$–$Pbnm$).[1,2] The distortion from the ideal perovskite is mainly in the positions of the R^{3+} ions, while the environment of the Fe^{3+} ion remains essentially octahedral. Each unit cell contains

† Research sponsored in part by the Air Force Materials Laboratory Research and Technology Division AFSC through the European Office of Aerospace Research, U. S. Air Force, under Contract No. F61052-67C-0040.

[1] D. Treves, J. Appl. Phys. **36**, 1033 (1965); Phys. Rev. **125**, 1843 (1963), and references cited therein.
[2] M. Eibschütz, S. Shtrikman, and D. Treves, Phys. Rev. **156**, 562 (1967).

four equivalent iron ions, but the axes of the four surrounding octahedra are slightly tilted with respect to each other. Previous studies[1,2] of the orthoferrites have shown that the iron ions are essentially antiferromagnetic in the ordered state, and that their arrangement can be described by two cubic interpenetrating sublattices in which each iron ion is surrounded by six nearest-neighbor antiferromagnetic ions. The weak ferromagnetic moment results from a small canting between the sublattices. Magnetic studies[1] have shown that in several orthoferrites this canting is governed by a Dzyaloshinsky-Moriya antisymmetric exchange mechanism. $YFeO_3$ is an example of this case. It has been shown that the canting angle is practically constant as a function of temperature.[2]

In most of the orthoferrites the rare-earth ions are paramagnetic (at sufficiently high temperatures) and give an appreciable contribution to the magnetic susceptibility of the material. In $YFeO_3$, however, the Y ions are diamagnetic, and if we neglect the diamagnetic contribution, the magnetic susceptibility is due only to the iron ions (Fe^{3+}, $S=\frac{5}{2}$). Thus, a study of the magnetic susceptibility in the relatively simpler case of $YFeO_3$ may eventually lead to a better understanding of the interactions existing in the other orthoferrites in which the rare-earth ions are paramagnetic. Experimental studies of magnetic properties of $YFeO_3$ have already been carried out.[1,3] However, the theoretical treatment in those studies is confined to absolute zero temperature only.

In this paper we report theoretical and experimental studies of the temperature dependence of the magnetic susceptibility parallel and perpendicular to the antiferromagnetic axis (the crystallographic x axis) in $YFeO_3$. The behavior near the transition temperature is also discussed. We consider also the nonlinear effect of an external magnetic field on the magnetization.

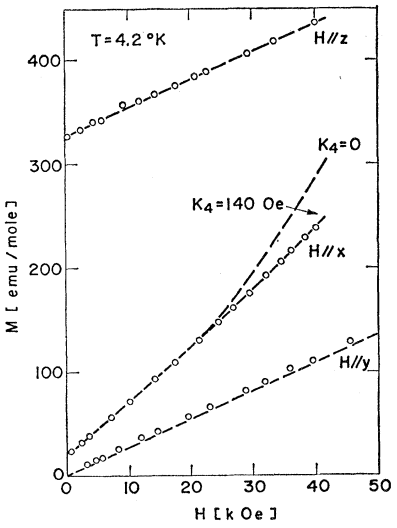

FIG. 1. Magnetization as a function of magnetic field applied along the principal crystallographic axes. The measurements were carried out at 4.2°K. The circles and dashed line denote experimental and theoretical results, respectively.

II. EXPERIMENTAL

The magnetization and susceptibility of a single crystal of $YFeO_3$ were measured along its orthorhombic axes at 4.2°K and between 90 and 1000°K.[4] The measurements at 4.2°K were carried out using a motor-driven vibrating sample magnetometer in which the magnetic field of a superconducting coil was applied parallel to the axis of vibration and the axis of the pickup coils. During the measurements the vibrating sample was immersed in the liquid-helium bath. The magnetization curves versus magnetic field up to 50 kOe are shown in Fig. 1.

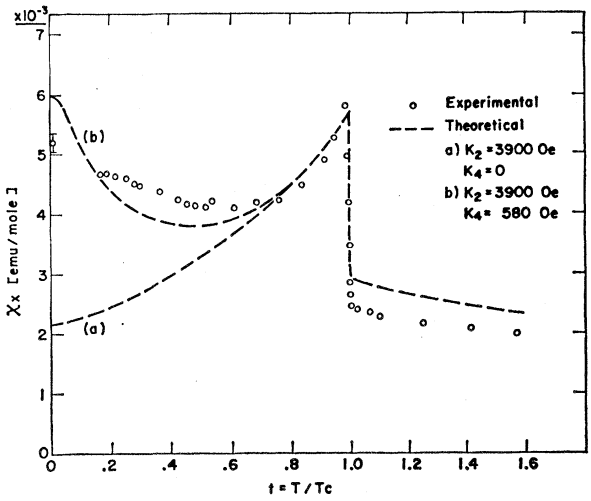

FIG. 2. Measured (circles) and calculated (dashed line) susceptibility parallel to x axis versus temperature.

The susceptibility above 85°K was measured by a similar method wherein a constant magnetic field was applied perpendicular to the direction of the vibration[5] while the sample was surrounded by a cryostat or a heater. The results are shown in Figs. 2 and 3. Figure 2 shows the susceptibility in the direction of the antiferromagnetic axis (x axis).

Figure 3 shows the susceptibility in directions perpendicular to the antiferromagnetic axis. It should be noted that the susceptibility along the y axis does not indicate any anomaly at the Curie point T_c, whereas for the susceptibility along the weak ferromagnetic moment a typical peak was observed. Its width above T_c, $\Delta T \simeq 1$°K, is in agreement with that

[3] V. M. Judin, A. B. Sherman, and I. E. Myl'nikova, Phys. Letters **22**, 554 (1966).

[4] The single crystals of $YFeO_3$ were kindly provided by Dr. J. P. Remeika, Bell Telephone Laboratories, Murray Hill, N. J.

[5] S. Foner, Rev. Sci. Instr. **30**, 548 (1956).

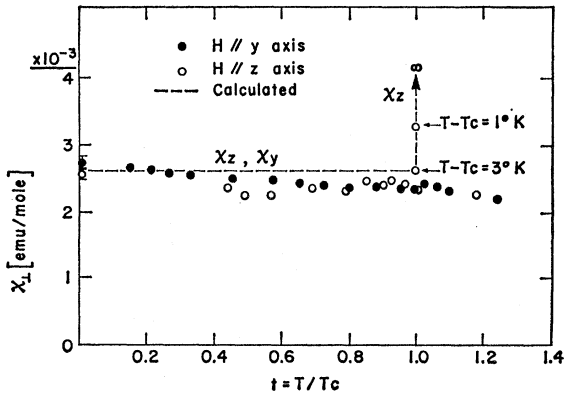

FIG. 3. Measured and calculated susceptibility in the y and z direction. The experimental value of χ_z at T_c is about 2.6×10^{-2} emu/mole for $H=170$ Oe. (See Ref. 5.)

observed by Gorodetsky *et al.*[6] and it is an order of magnitude smaller than that reported previously.[3]

III. THEORY

The main purpose of the present theoretical treatment is to account in a semiquantitative manner for the salient features of the experimental results. We thus adopt a relatively simple Hamiltonian and employ the molecular-field approximation.

In the two-sublattice description of the iron spins, let the plus sublattice be the sublattice of the spins which lie essentially in the $+x$ direction and the minus sublattice that of spins in the $-x$ direction.

The Hamiltonian of the Fe^{3+} spins in a unit volume can be written

$$\mathcal{H}=2J\sum_{\langle ij\rangle}\mathbf{S}_i\cdot\mathbf{S}_j-\mathbf{D}\cdot\sum_{\langle ij\rangle}\mathbf{S}_i\times\mathbf{S}_j-K_2{}^1\sum_l S_{lx}{}^2 +K_4{}^1\sum_l(S_{lx}{}^4+S_{ly}{}^4+S_{lz}{}^4)-g\mu_B\mathbf{H}\cdot\sum_l\mathbf{S}_l, \quad (1)$$

where $\mathbf{S}_i$ is a spin in the plus sublattice, $\mathbf{S}_j$ belongs to the minus sublattice, $\mathbf{S}_l$ belongs to either one of the sublattices, the l summation extends over all spins, and the $\langle ij\rangle$ summation extends over pairs of nearest-neighbor spins. The first and second terms are the isotropic nearest-neighbor and Dzyaloshinsky-Moriya exchange interactions, respectively. The third term is a uniaxial anisotropy which fixes the crystallographic x axis as the easy direction for each sublattice, namely, the antiferromagnetic axis. The fourth term is a cubic anisotropy which is included in anticipation of its effect on the parallel susceptibility. The last term is the direct interaction of the spin with the external magnetic field. The Dzyaloshinsky vector D is in the $-y$ direction[1] and in the absence of an external magnetic field the spins of both sublattices are confined to lie in the crystallographic xz plane. The coefficient K_2' depends on temperature like $\langle S_x{}^2\rangle-\frac{1}{3}S(S+1)$, where $\langle\ \rangle$ means a thermal average. The temperature dependence of the cubic term is given by Wolf.[7] In the molecular-field approximation the Hamiltonian can be written

$$\mathcal{H}=-g\mu_B\mathbf{H}^+\cdot\sum_i\mathbf{S}_i-g\mu_B\mathbf{H}^-\cdot\sum_j\mathbf{S}_j, \quad (2)$$

where $\mathbf{H}^+$ and $\mathbf{H}^-$ are the effective fields acting on a spin $\mathbf{S}_i$ in the plus sublattice and a spin $\mathbf{S}_j$ in the minus sublattice, respectively. $\mathbf{H}^\pm$ is given by

$$\mathbf{H}^\pm=-A\mathbf{M}^\mp\mp\mathbf{D}'\times\mathbf{M}^\mp+\mathbf{H}_a{}^\pm+\mathbf{H}, \quad (3)$$

where $\mathbf{M}^+=\frac{1}{2}Ng\mu_B\langle\mathbf{S}_i\rangle$ and $\mathbf{M}^-=\frac{1}{2}Ng\mu_B\langle\mathbf{S}_j\rangle$ are the plus and minus sublattice magnetization per unit volume (N being the number of spins per unit volume), $A=4Jz/Ng^2\mu_B{}^2$, $\mathbf{D}'=2zD/Ng^2\mu_B{}^2$, z $(=6)$ is the number of nearest neighbors, and $\mathbf{H}_a{}^\pm$ is the anisotropy field: $H_{ax}{}^\pm=\pm H_a$ and $H_{ay}{}^\pm=H_{az}{}^\pm=0$.

A. Susceptibility below T_c

1. Parallel Susceptibility χ_x

In this case $H_x=H$ and $H_y=H_z=0$. The spins of both sublattices remain in the xz plane even in presence of the external magnetic field. Thus $\mathbf{H}^\pm$ is also in the xz plane, and since $D_x'=D_z'=0$ and $D_y'=-D'$, the components of $\mathbf{H}^\pm$ are given by

$$\begin{aligned}H_x{}^\pm&=-AM_x{}^\mp\pm D'M_z{}^\mp\pm H_a+H,\\ H_y{}^\pm&=0,\\ H_z{}^\pm&=-AM_z{}^\mp\mp D'M_x{}^\mp.\end{aligned} \quad (4)$$

We now expand $M_x{}^\pm$ and $M_z{}^\pm$ up to first order in powers of H. The zero-order terms, namely, the components of the sublattice magnetization in the absence of the magnetic field which we designate by the subscript 0, are

$$\begin{aligned}M_{0x}{}^+&=-M_{0x}{}^-=M_{0x},\\ M_{0z}{}^+&=M_{0z}{}^-=M_{0z}.\end{aligned} \quad (5)$$

Symmetry considerations indicate that the expansions are

$$\begin{aligned}M_x{}^\pm&=\pm M_{0x}+aH,\\ M_z{}^\pm&=M_{0z}\mp bH.\end{aligned} \quad (6)$$

The coefficient a determines the susceptibility. From (6) follows

$$M^\pm=[(M_x{}^\pm)^2+(M_z{}^\pm)^2]^{1/2} =M_0\pm[(M_{0x}a-M_{0z}b)/M_0]H, \quad (7)$$

where $M_0=(M_{0x}{}^2+M_{0z}{}^2)^{1/2}$ is the sublattice magnetization in the absence of the external field. Substitution of (6) into (4) yields

$$H^\pm=[(H_x{}^\pm)^2+(H_z{}^\pm)^2]^{1/2}=H_0{}^\pm(d/H_0)H, \quad (8)$$

[6] G. Gorodetsky, S. Shtrikman, and D. Treves, Solid State Commun. 4, 147 (1966).

[7] W. P. Wolf, Phys. Rev. 108, 1152 (1957).

where H_0, the effective field in the absence of the external magnetic field, is given by

$$H_0=[(A^2+D'^2)M_0^2+H_a^2+(2AM_{0x}+2D'M_{0z})H_a]^{1/2} \quad (9)$$

and

$$d=AM_{0x}+D'M_{0z}+H_a-[(A^2+D'^2)M_{0x}+AH_a]a +[(A^2+D'^2)M_{0z}+D'H_a]b. \quad (10)$$

The equilibrium conditions require that each spin lies in the direction of the effective field acting on it. This requirement can be expressed as

$$M_x^{\pm}/H_x^{\pm}=M_z^{\pm}/H_z^{\pm}. \quad (11)$$

Substituting Eqs. (4) and (6) into (11) and then comparing powers of H, we obtain the following equations. From the zero-order term we obtain

$$2AM_{0x}M_{0z}+D'(M_{0z}^2-M_{0x}^2)+M_{0z}H_a=0. \quad (12)$$

From the coefficient of H we obtain

$$M_{0z}-H_ab=0. \quad (13)$$

In order to find another equation for a and b, we proceed as follows: The sublattice magnetization is given in the molecular-field approximation by the Brillouin function, namely,

$$M^{\pm}=M(0)B_S(y^{\pm}), \quad (14)$$

where $M(0)=\frac{1}{2}Ng\mu_BS$ is the saturation sublattice magnetization, and

$$y^{\pm}=g\mu_BSH^{\pm}/kT=y_0\pm(g\mu_BSd/H_0kT)H, \quad (15)$$

where

$$y_0=g\mu_BSH_0/kT. \quad (16)$$

k is Boltzmann's constant, and T is the absolute temperature. Let us expand $B_S(y^{\pm})$ in powers of H around y_0. Then Eq. (14) becomes

$$M^{\pm}=M_0\pm[M(0)g\mu_BB_S'(y_0)d/H_0kT]H. \quad (17)$$

B_S' is the derivative of B_S with respect to its argument. Comparing Eqs. (17) and (7) and using Eqs. (10) and (13), we obtain an equation for a. The result for the susceptibility per unit volume is

$$\chi_x=2a=\frac{Ng^2\mu_B^2S^2M_0B_S'(y_0)[(AM_{0x}+2D'M_{0z}+H_a)H_a+(A^2+D'^2)M_{0z}^2]+2M_{0z}^2H_0kT}{\frac{1}{2}Ng^2\mu_B^2S^2M_0B_S'(y_0)[(A^2+D'^2)M_{0x}+AH_a]H_a+M_{0x}H_aH_0kT}. \quad (18)$$

2. Susceptibility in the z Direction χ_z

In this case, $H_x=H_y=0$ and $H_z=H$. The spins of both sublattices remain in the xz plane. The expressions for $H_x^{\pm}$ and $H_z^{\pm}$ are the same as in Eq. (4) except that now H appears in $H_z^{\pm}$ instead of $H_x^{\pm}$. The expansions analogous to Eq. (6) are

$$M_x^{\pm}=\pm M_{0x}\mp\alpha H, \quad M_z^{\pm}=M_{0z}+\beta H. \quad (19)$$

The coefficient β determines the susceptibility. Following the same procedure as in the parallel case, we obtain for the susceptibility

$$\chi_z=2\beta=\{Ng^2\mu_B^2S^2M_0B_S'(y_0)[2A^2M_{0z}^2+(D'^2-A^2)M_{0x}^2 -4AD'M_{0x}M_{0z}-AM_{0x}H_a]+2M_{0x}^2H_0kT\}/ \{\tfrac{1}{2}Ng^2\mu_B^2S^2M_0B_S'(y_0)[(A^2+D'^2) \times(2A(M_{0z}^2-M_{0x}^2)-4D'M_{0x}M_{0z}-3M_{0x}H_a) -AH_a^2]+[2A(M_{0x}^2-M_{0z}^2) +4D'M_{0x}M_{0z}+M_{0x}H_a]H_0kT\}. \quad (20)$$

3. Susceptibility in the y Direction

In this case $H_x=H_z=0$ and $H_y=H$. The spins rotate out of the xz plane. Now

$$H_x^{\pm}=-AM_x^{\mp}\pm D'M_z^{\mp}\pm H_a, \quad H_y^{\pm}=-AM_y^{\mp}+H, \quad H_z^{\pm}=-AM_z^{\mp}\mp D'M_x^{\mp}, \quad (21)$$

and the expressions analogous to Eq. (6) are

$$M_x^{\pm}=\pm M_{0x}+O(H^2), \quad M_y^{\pm}=cH, \quad M_z^{\pm}=M_{0z}+O(H^2). \quad (22)$$

The coefficient c determines the susceptibility. The calculation now yields

$$\chi_y=2c=2M_{0z}/(2AM_{0x}+D'M_{0z}+H_a) =2M_{0z}/D'M_{0x}. \quad (23)$$

The last equality follows from Eq. (12).

B. Susceptibility above T_c

In this section we calculate the paramagnetic susceptibility χ_z parallel to the weak ferromagnetic direction. Ignoring anisotropy, χ_y is the usual paramagnetic susceptibility of a pure antiferromagnetic and $\chi_z=\chi_z$.

The effective field components $H_x^{\pm}$ and $H_z^{\pm}$ are the same as in the magnetic region (with H_a taken as zero) but now

$$M_x^{\pm}=\pm\gamma H, \quad M_z^{\pm}=\delta H. \quad (24)$$

The coefficient δ determines the susceptibility. We now expand (14) around $y=0$ and get

$$\chi_z=Ng^2\mu_B^2S(S+1)\frac{3kT-\frac{1}{2}Ng^2\mu_B^2S(S+1)A}{9k^2(T^2-T_c^2)}, \quad (25)$$

where

$$T_c=Ng^2\mu_B{}^2S(S+1)(A+D'^2)^{1/2}/6k \tag{26}$$

is the transition temperature.

C. Nonlinear Field Dependence of the Magnetization at $T=0°K$

In this section we calculate the nonlinear dependence of the magnetization on an external magnetic field applied along one of the crystal axes for $T=0°K$. This dependence is derived up to third-order terms in the field, in view of the experimentally observed departure from linearity in the case of $\mathbf{H}\|x$ which is asymmetric with respect to the field. Second-order terms are eliminated by symmetry in the case of $\mathbf{H}\|x$ or $\mathbf{H}\|y$.

The Hamiltonian (1) for a pair of spins can be written for $T=0°K$ and $\mathbf{H}\|x$ as

$$\begin{aligned}\mathcal{H}=&-2JzS^2\cos(\alpha+\beta)-DzS^2\sin(\alpha+\beta)\\&-k_2(\cos^2\alpha+\cos^2\beta)-k_4(\sin^22\alpha+\sin^22\beta)\\&-g\mu_BHS(\cos\alpha-\cos\beta),\end{aligned} \tag{27}$$

where α and β are the canting angles of the two sublattices, H is the external magnetic field in the x direction, and k_4 is a cubic anisotropy term.

Minimizing this Hamiltonian with respect to α and β and expanding

$$\begin{aligned}\sin\tfrac{1}{2}(\alpha+\beta)&=b_0+b_2H^2,\\ \sin\tfrac{1}{2}(\alpha-\beta)&=a_1H+a_3H^3,\end{aligned} \tag{28}$$

we obtain for the magnetization M_x

$$\begin{aligned}M_x=&\frac{Ng^2\mu_B{}^2S^2D^2}{32J^2(k_2-4k_4)^2}H+Ng^4\mu_B{}^4S^4\Bigg(\frac{D^2}{128J^3S^2z(k_2-4k_4)^2}\\&-\frac{k_4D^4}{256J^4(k_2-4k_4)^4}\Bigg)H^3.\end{aligned} \tag{29}$$

In obtaining Eq. (29) we assumed that D, k_2, and k_4 are small compared to J, and smaller terms than those given were neglected.

In the case of $\mathbf{H}\|y$ the Hamiltonian after neglecting the anisotropy term is

$$\begin{aligned}\mathcal{H}=&-2JzS^2\cos2\alpha-DzS^2\sin2\alpha\cos\gamma\\&-2g\mu_BSH\sin\alpha\sin\gamma,\end{aligned} \tag{30}$$

where α is the canting angle of each spin from the x axis and γ is the angle between the z axis and the projection of each spin in the yz plane. Minimizing with respect to α and γ and expanding

$$\begin{aligned}\sin\alpha&=A_0+A_2H^2,\\ \sin\gamma&=B_1H+B_3H^3,\end{aligned} \tag{31}$$

we obtain for the magnetization $M_y(H)$

$$M_y=\frac{Ng^2\mu_B{}^2}{4Jz}H+\frac{Ng^4\mu_B{}^4}{128JD^2z^3S^2}H^3\times O\left(\frac{D^2}{J^2}\right). \tag{32}$$

In the case of $\mathbf{H}\|z$ the Hamiltonian is

$$\mathcal{H}=-2JzS^2\cos2\alpha-DzS^2\sin2\alpha-2g\mu_BSH\sin\alpha. \tag{33}$$

Minimizing with respect to α and expanding

$$\sin\alpha=A_0+A_1H+A_2H^2+A_3H^3, \tag{34}$$

we obtain for $M_z(H)$

$$\begin{aligned}M_z=&\frac{NDg\mu_BS}{4J}+\frac{Ng^2\mu_B{}^2}{4Jz}H-\frac{3NDg^3\mu_B{}^3}{128J^3z^2S}H^2\\&+\frac{3ND^2g^4\mu_B{}^4}{8192J^5z^3S^2}H^3\times O\left(\frac{D^2}{J^2}\right).\end{aligned} \tag{35}$$

IV. RESULTS AND DISCUSSION

A. Determination of Parameters

The exchange parameter J (or A) has been determined by fitting Eqs. (32) and (35) for $M_y(H)$ and $M_z(H)$ to the experimental data. The value obtained is $J=23.3°K$ and $A=1.26\times10^4$.[8] From Eq. (12) one obtains, after neglecting the anisotropy (which is small compared to the exchange),

$$\tan2\alpha=D'/A. \tag{36}$$

Since α is small, it follows that

$$\sin\alpha=D'/2A=D/4J; \tag{37}$$

$\sin\alpha$ is determined by fitting Eq. (35) for $H=0$ to the experimental value (Fig. 1), $\sin\alpha=0.012$, and D' is then determined from Eq. (37), which gives $D'=2.94\times10^2$.

The anisotropy field is given by

$$H_a=K_2\frac{\langle S_x{}^2\rangle/S^2-\frac{1}{3}(S+1)/S}{\langle S_x\rangle/S}-K_4\frac{|r|}{\langle S_x\rangle/S}, \tag{38}$$

where K_2 and K_4 are constants and r is a polynomial which gives the dependence of the cubic anisotropy on $\langle S_x\rangle/S$.[7] The first term is the uniaxial anisotropy—the p polynomial in Wolf's[7] paper. The temperature dependence of $\langle S_x\rangle/S$ is taken from Mössbauer effect measurements.[2] The values of K_2 and K_4 are determined by fitting the measured temperature dependence of the susceptibility χ_x to Eq. (18). The result for two sets of K_2 and K_4 is compared with experiment in Fig. 2. For $K_2=3900$ Oe and $K_4=580$ Oe qualitative agreement between theory and experiment is obtained. The importance of the cubic anisotropy is demonstrated by the case $K_4=0$, which exhibits a clear discrepancy between theory and experiment at low temperatures. The K_4 term vanishes much stronger than the K_2 term when T approaches T_c. At low temperatures the K_4 term is quite appreciable, and since the easy direction

[8] This value is obtained using the lattice constants for $YFeO_3$ given by M. Eibschütz, Acta Cryst. **19**, 337 (1965).

for the cubic anisotropy is 45° from that of the uniaxial (the x axis), the effective anisotropy field in the x direction is reduced and the susceptibility increases. The importance of the cubic anisotropy in other orthoferrites was already recognized by Gyorgy *et al.*[9] in $SmFeO_3$ and by Shane[10] in $TmFeO_3$. Both our experimental results and theoretical interpretation differ from the results of Judin *et al.*,[3] wherein χ_x is constant throughout the whole temperature range.

The quantities K_2 and K_4 were also determined by fitting the measured $M_x(H)$ at 4.2°K to Eq. (29). The values obtained for k_2 and k_4 appearing in (29) are $k_2=2.55\times10^{-17}$ erg and $k_4=2\times10^{-18}$ erg. The relation between k_2, k_4 and K_2, K_4, respectively, which can be obtained, for example, by comparing Eq. (18) at $T=0$°K with Eq. (29), is

$$K_2=15k_2/4g\mu_BS, \quad K_4=16k_4/5g\mu_BS. \tag{39}$$

With these relations and the value of k_2 and k_4 one obtains $K_2=2070$ Oe and $K_4=140$ Oe.

The measured and calculated $M(H)$ are given in Fig. 1. The measured $M(H)$ were obtained at $T=4.2$°K and magnetic fields up to 50 kOe.

$M_y(H)$ and $M_z(H)$ are straight lines and no nonlinearity is observed. For example, the contributions of the H^2 and H^3 terms to $M_z(H)$ for $H\sim50$ kOe are less than 1% and about 10^{-10}, respectively, of that of the susceptibility. The contribution of the H^3 term to $M_y(H)$ is 10^{-5}–10^{-4} of that of the susceptibility for $H\sim50$ kOe.

The measured $M_x(H)$ and $M_y(H)$ are small but finite even for $H=0$. This is due to that H was not exactly in the x or y direction, and thus a small component of the ferromagnetic moment was present.

In Fig. 3 are given the measured and calculated perpendicular susceptibilities χ_y and χ_z as a function of temperature. The behavior of χ_z near T_c is discussed in the next paragraph. The calculated χ_y and χ_z are practically equal and constant. The slight discrepancy between theory and experiment in the region below T_c may be attributed to the molecular-field approximation. A more accurate statistical theory might reduce this discrepancy as shown by Anderson and Callen.[11] Also, the discrepancy between calculated and measured susceptibility above T_c is due to the disadvantage of the molecular-field approximation which agrees qualitatively with experiment only in the high-temperature limit. We also ignored a single-ion uniaxial anisotropy, A_{xz} in Herman's notation,[12] which is allowed in principle by symmetry. The effect of this term on the canting angle is to yield $\sin\alpha=(D+A_{xz})/2A$. A_{xz} varies with temperature like our K_2 term. Since experiment indicates that the canting angle in our case does not vary with temperature,[2] A_{xz} is small compared to D. Furthermore, since A_{xz} varies like K_2, it will not account, if the cubic anisotropy term is not included, for the peculiar temperature dependence of χ_x. Since the salient experimental features are well described by our model, the A_{xz} term, which might have a relatively minor effect on our results, is not included.

B. Behavior near the Transition Point

The theory of weak ferromagnets shows that the susceptibility parallel to the weak ferromagnetic moment diverges as T approaches T_c from both sides.[13,14] This follows from our results too. Since χ_z is not very sensitive to the anisotropy H_a (as long as H_a is not too large), we neglect it in Eq. (20). M_0 then cancels out and by expanding $B_s'(y_0)$ in powers of y_0 we obtain

$$\chi_z=\frac{A(\cos^2\alpha-3\sin^2\alpha)(T_c-T)+A\sin^2\alpha T_c}{(A^2+D'^2)\cos2\alpha(T_c-T)}, \quad T<T_c; \tag{40}$$

$\cos\alpha$ and $\sin\alpha$ can be expressed in terms of A and D' using Eq. (36), and T_c is given by Eq. (26).

The paramagnetic susceptibility near T_c is

$$\chi_z=\frac{Ng^2\mu_B^2S(S+1)}{6kT_c}\left(1+\frac{T_c-Ng^2\mu_B^2S(S+1)A/6k}{T-T_c}\right), \quad T>T_c. \tag{41}$$

Assuming $D'\ll A$, we obtain

$$\begin{aligned}\chi_z&=\frac{Ng^2\mu_B^2S(S+1)}{6kT_c}\left(1+\frac{D'^2T_c}{4A^2(T_c-T)}\right), \quad T<T_c\\ \chi_z&=\frac{Ng^2\mu_B^2S(S+1)}{6kT_c}\left(1+\frac{D'^2T_c}{2A^2(T-T_c)}\right), \quad T>T_c.\end{aligned} \tag{42}$$

We see that the peak at T_c is asymmetric and $\chi(T_c+\Delta T)=2\chi(T_c-\Delta T)$. This result is the same obtained by the Landau theory of phase transitions[13,14] with similar conditions on the ratio between the parameters. It is worth noting that the same relation is obtained also in the case of $A=0$, while in the general case there is no such simple relation.

[9] E. M. Gyorgy, J. P. Remeika, and F. B. Hagedorn, J. Appl. Phys. **39**, 1369 (1968).
[10] J. R. Shane, Phys. Rev. Letters **20**, 728 (1968).
[11] F. B. Anderson and H. B. Callen, Phys. Rev. **136**, A1068 (1964).
[12] G. F. Herman, Phys. Rev. **133**, A1334 (1964).
[13] T. Moriya, in *Weak Ferromagnetism, Magnetism*, edited by G. T. Rado and H. Suhl (Academic Press Inc., New York, 1963), Vol. 1, p. 85.
[14] A. S. Borovik-Romanov and V. I. Ozhogin, Zh. Eksperim. i Teor. Fiz. **39**, 27 (1960) [English transl.: Soviet Phys.—JETP **12**, 18 (1961)].